Published in final edited form as:
Nano Lett. 2012 November 14; 12(11): 5532–5538. doi:10.1021/nl302412f.

DETERMINING THE PHARMACOKINETICS AND LONG-TERM BIODISTRIBUTION OF SiO_2 NANOPARTICLES *IN VIVO* USING ACCELERATOR MASS SPECTROMETRY

Michael A. Malfatti[1,2], **Heather A. Palko**[1,2], **Edward A. Kuhn**[1], and **Kenneth W. Turteltaub**[1,2]

[1]Biosciences and Biotechnology Division, Physical and Life Sciences Directorate Lawrence Livermore National Laboratory, Livermore, CA

[2]Battelle Center for Fundamental and Applied Systems Toxicology (B-FAST) Battelle, Columbus, OH

Abstract

Biodistribution is an important factor in better understanding silica dioxide nanoparticle (SiNP) safety. Currently, comprehensive studies on biodistribution are lacking, most likely due to the lack of suitable analytical methods. Accelerator mass spectrometry (AMS) was used to investigate the relationship between administered dose, PK, and long-term biodistribution of ^{14}C-SiNPs *in vivo*. PK analysis showed that SiNPs were rapidly cleared from the central compartment, were distributed to tissues of the reticuloendothelial system, and persisted in the tissue over the 8-week time course, raising questions about the potential for bioaccumulation and associated long-term effects.

Keywords

accelerator mass spectrometry; silica nanoparticles; pharmacokinetics; biodistribution; bioaccumulation

The increasing use of nanoparticles (NPs) for a wide variety of commercial, industrial, and biomedical applications has led to concerns about their safety. Because of their unique properties such as monodispersity, large surface area, and high drug loading efficiency,[1, 2] silica nanoparticles (SiNPs) have been developed for a vast array of biomedical uses such as optical imaging,[3] cancer therapy,[4] targeted drug delivery[5] and controlled drug release for genes and proteins.[6, 7] Silica nanoparticles are also found in many personal care products and in certain foods[8]. However, as the potential uses of SiNPs have increased, the evaluation of their biological fate and toxicity has not kept pace[9]. Currently, a complete understanding of the size, shape and composition-dependent interactions of SiNPs with biological systems is lacking,[10] and thus it is unclear whether these particles can elicit a toxic biological response.[11] Understanding the dosimetry of these particles and what factors affect bioavailability is an important component of this evaluation. A systematic and thorough quantitative analysis of the absorption, distribution, elimination, and pharmacokinetics (PK) is needed for a better understanding of SiNP interactions with tissues and cell types, and for assessments of basic distribution and clearance that serve as the basis in determining whether there is a potential for an exposure hazard.

Corresponding author: Michael A. Malfatti, PhD, Biosciences and Biotechnology Division, Lawrence Livermore National Laboratory, 7000 East Avenue, L-452, Livermore, CA 94550, Phone: 925-422-5732, malfatti1@llnlgov.

Previous studies have shown that the inhalation of microscale crystalline silica is potentially linked with the pulmonary disease silicosis in humans.[11] Chronic inhalation studies in rats have been associated with pulmonary fibrosis and cancer.[12] Exposure to microscale amporphous silica has been linked to inflammation, granuloma formation and emphysema. [13] It is likely that the unique properties of SiNPs may impose different biological effects than what has been reported from microscale particles. Thus, the biological fate of SiNPs warrants further investigation. In contrast to a significant number of studies that have reported on the biological fate of other nanoparticles such as quantum dots,[14, 15] liposomes,[16, 17] and carbon nanotubes,[18, 19] studies on the quantitative biodistribution and PK of SiNPs are lacking. This is likely due to the lack of suitable analytical methods.

Most studies to date that have investigated *in vivo* biodistribution of SiNPs have relied on fluorescence detection techniques and have been qualitative in nature.[20–23] In all these studies, results showed that SiNPs distributed primarily to the liver and spleen. Cho *et al.* showed that SiNPs, when administered to mice intravenously (IV), induced an inflammatory response in the liver and were retained in both the liver and spleen up to 4 weeks after dosing.[20] Likewise, He *et al.* reported, using fluorescence intensity measurements, that mesoporous silica distribute mainly to the liver and spleen with small quantities being found in the lung, kidney, and heart.[21] Furthermore, in a study using ^{125}I-labeled SiNPs, Xie *et al.* reported that SiNPs administered IV to mice accumulate mainly in the lungs, liver, and spleen, and are retained for 30 days in the tissue.[9] Additional studies have also shown that shape, size, and surface characteristics can affect biodistribution, bioaccumulation, and PK of SiNPs. Yu *et al.* demonstrated that silica nanorods showed enhanced lung bioaccumulation compared to silica nanaospheres, and accumulation was reduced by primary amine modification.[24] Spherical mesoporous silica nanoparticles (80–120 nm diameter) with surface pegylation had lower capture by the reticuloendothelial system (RES), had a longer blood circulation half life, and were more slowly biodegraded compared to nonpegylated particels of the same size.[21] Additionally, organically modified silica nanoparticles with diameters of 20–25 nm exhibited effective clearance via the hepatobiliary route without any sign of organ toxicity after a 15 days.[25] As these studies contribute to the understanding of SiNP biodistribution, showing that SiNPs distribute mainly to tissues of the RES, comprehensive, quantitative long-term biodistribution and pharmacokinetic studies are still needed to better understand the relationship between administered dose, biological fate, and ultimate toxicity.

In the current study, the PK properties and the quantitative long-term tissue distribution of amporphous spherical ^{14}C-SiNPs, was investigated using the technique of accelerator mass spectrometry (AMS). AMS is a technique for the measurement of rare, long-lived isotopes with extremely high sensitivity. AMS counts isotopes independent of radioactive decay by measuring the mass ratio of the radioisotope of interest relative to a stable isotope of the element. AMS can be used to trace the fate of any molecule in *in vitro* systems or whole organisms if it is labeled with an isotope appropriate for AMS analysis. Because most biological materials contain carbon, the majority of biological AMS studies use ^{14}C as the radiotracer. AMS can detect and quantify a ^{14}C-labeled compound in a biological matrix with 1%–3% precision at levels ranging from approximately 10 pmol ^{14}C to 1 attomol (1×10^{-18}) ^{14}C in samples containing 1 mg of total carbon.[26, 27] Studies with AMS in laboratory animals to determine the kinetics of absorption, distribution, and excretion, and to identify and quantify metabolites using chemical doses of 0.1 to 500 ng/kg body weight and radioisotope doses of under 10 nCi/kg have been routinely carried out. [28, 29] The sensitivity of AMS measurement gives this technique a number of major advantages over other methods for the detection of isotopes. Importantly, because of the extreme sensitivity, PK studies have the ability to determine long-term kinetics and metabolism using low doses for

several months after isotope administration. Furthermore, since only low doses of chemical and radioactivity are required, studies can be performed with levels of chemicals equivalent to therapeutic or environmental exposures. This is a significant feature because the biological effects observed at high doses may not extrapolate to the low doses that are typically encountered in real exposure scenarios. In addition, detailed pharmacokinetic data require frequent sampling, which is made possible with AMS detection, by virtue of the small sample sizes needed for analysis. AMS has been used to establish the kinetics of β-carotene uptake and plasma clearance in a human volunteer who received a single dose of ^{14}C-β-carotene obtained from ^{14}C labeled spinach.[30]. Plasma concentrations of β-carotene and its metabolites were determined at intervals over a 7-month period and required just 30 μl of plasma/analysis. Such complete investigations would not be possible using other methods that lack the necessary sensitivity to detect compounds and metabolites months after dosing.

While AMS has been used extensively in the study of chemical dosimetry, it has not yet been applied to the study of nanoparticles. To assess the suitability of AMS as a technique to evaluate the PK and long-term tissue distribution of SiNPs, mice were dosed (IV) with a single injection of ^{14}C-SiNPs and blood and tissues were collected at specified time intervals after SiNP administration. Because of the high sensitivity and precision of AMS, it was possible to track the SiNPs out to 8 weeks post exposure. The decision to end the study at 8 weeks was arbitrary, and was not limited due to the detection limits of AMS. In fact, the results suggest that AMS is capable of detecting the SiNPs for perhaps up to several months after exposure.

The amporphous spherical ^{14}C-labeled SiNPs and unlabeled SiNPs used for the study were provided by Oak Ridge National Laboratory, Oak Ridge, TN. Synthesis of the ^{14}C-labeled and unlabeled SiNPs was achieved by, hydrolyzing tetraethoxysilane with NH_3 as a catalyst in microemulsion media [31] based on the Stober method, [32] described in detail elsewhere. To introduce the ^{14}C isotope into SiO_2, ^{14}C-acrylic acid was used as a ^{14}C precursor. The ^{14}C-acrylic acid (2.5mg, 62.5μCi) and 0.46g allyltrimethoxysilane was first added into the microemulsion under magnetic stirring, and then 0.2mL of saturated $(NH_4)_2S_2O_8$ solution was added. With $(NH_4)_2S_2O_8$ as initiator, the ^{14}C was chemically grafted into a silane agent through radical induced polymerization between the ^{14}C-acrylic acid and allyltrimethoxysilane (unpublished data). This procedure resulted in ^{14}C-SiNPs with a specific activity of 0.23 nCi/mg and an average diameter of 33 nm. The SiNPS were approximately 3 months old at the time of use.

Biological stability of the ^{14}C-SiNPs was evaluated in saline and fetal bovine serum (FBS, Gibco, Invitrogen) over 8 weeks. No significant loss of ^{14}C- label was observed for either solution, indicating that the labeled particles remained intact over the study period (unpublished data).

For the biodistribution and PK studies, six to eight week old male BALB/c mice (n=5 per time point) were administered a single intravenous dose of 0.5 mg ^{14}C-SiO_2 nanoparticles through an implanted jugular vein catheter. To ensure the SiNPS were well dispersed, they were sonicated for 30 min in a water bath sonicator prior to injection. The nanoparticle injection was immediately followed by an injection of 50 μl of saline into the catheter to ensure complete infusion of the nanoparticle solution into the blood stream. Animals were housed individually in polystyrene cages containing hardwood bedding and kept on a 12 h light/dark cycle in a ventilated room maintained at 24°C in an AAALAC accredited facility. Experiments were conducted following all the guidelines and regulations set by Lawrence Livermore National Laboratory and with IACUC approval. At designated time points up through eight weeks animals were euthanized by CO_2 asphyxiation. A subset of animals was

placed in metabolism cages and urine and feces were collected over the first 24 h after ^{14}C-SiNP administration. Following euthanasia and subsequent open thoracotomy, blood was collected via cardiac puncture, and tissues were harvested. Whole blood was placed into Microtainer® tubes coated with lithium heparin (Bectin Dickinson, Franklin Lakes, NJ) and placed on ice. Plasma was separated from the whole blood by centrifugation (10,000 × g for 2 min) within 1 hour of collection, the volume recorded, and stored at −80°C until analysis. Tissues were excised from the carcass, rinsed twice in phosphate buffered saline (PBS), placed in pre-weighed glass vials (28 × 60 mm), and immediately frozen at −20° C until analysis. Clean unused surgical tools were used for each animal to avoid cross contamination of radiocarbon. Tissues collected included liver, spleen, kidney, lung, heart, bone marrow, upper gi, colon, muscle, adipose, brain, and cervical lymph nodes.

Not only was this the first study to use AMS to quantitatively track nanoparticles *in vivo*, it is also the first to use AMS to measure a nonsoluble test article. The SiNPs used in the study do not breakdown and do not solubilize in a biological matrix. Because of this, tissue homogenization methods were developed to ensure there was a uniform sampling distribution of SiNPS within each tissue that was compatible with AMS analysis. To homogenize the tissues each tissue type was incubated in 1–2 ml of a 0.11 M KCl based buffer, containing 3.4 mM NaCl, 0.4 mM $MgSO_4$, 40 mM $CaCl_2$, 4 mg/ml type IV collagenase, and 1.1 U/ml DNAse 1. Samples were incubated overnight at 37°C in a shaking water bath with gentle agitation. After the incubation time, samples were vortexed vigorously for 1–3 min to break up any solid particles to ensure complete digestion of the tissues. An aliquot of each homogenate was subsequently analyzed for radiocarbon content by AMS.

Preparation of the samples for radiocarbon analysis by AMS requires conversion of the samples to graphite. This procedure has been described previously.[33] Briefly, all the tissues and reagents were handled carefully to avoid radiocarbon cross-contamination. This required using disposable materials for any item that might come into contact with the samples. A 30–50 μl aliquot of each tissue homogenate was pipetted into 6 × 55 mm quartz tubes using aerosol resistant tips. For small samples such as bone marrow and lymph tissue, 1 mg of carbon in the form of tributyrin (carrier carbon) was added to the samples to bring the total carbon content to 1 mg (this provided the optimal amount of carbon for efficient conversion to graphite). All samples were subsequently dried under vacuum centrifugation. The dried samples were then converted to graphite by a two-step process using reported methods.[34] Briefly, the dried samples were oxidized to CO_2 by heating at 900° C for 4 h in the presence of copper oxide. The CO_2 was then cryogenically transferred to a septa-sealed vial under vacuum and reduced to filamentous graphite in the presence of cobalt, titanium hydride, and zinc powder.

To determine SiNP concentration in the tissues homogenagtes, plasma and excreta the radiocarbon content of each sample was determined by AMS as described previously.[34–36] The $^{14}C/^{12}C$ ratios from the graphitized samples obtained by AMS were converted to μg SiNPs per mg tissue or ml of plasma/urine after subtraction of the background carbon contributed from the sample and carrier carbon, and correction for the specific activity of the ^{14}C-SiNPs, and the carbon content of the sample. [26] The carbon content of each tissue was determined using a CE-440 elemental analyzer (Exeter Analytical, Inc. North Chelmsford, MA). Tissues were determined to have a carbon content ranging between 10%–15%. Plasma carbon content was 3.8% and urine carbon content was variable between 0.5%–3%.

The pharmacokinetic parameters of SiNPs in plasma were determined by non-compartmental analysis using PK Solutions Software (Summit Research Services, Montrose,

CO). The concentration of SiNPs over time was determined by quantifying the amount of ^{14}C-SiNP equivalents at each time points, by AMS, and constructing concentration vs. time curves. Figure 1 depicts the plasma ^{14}C-SiNP concentration versus time data over 48 h following intravenous administration of ^{14}C-SiNP in mice. Based on ^{14}C equivalents, the SiNPs were rapidly cleared from the central compartment following first order processes with a mean distribution half-life ($t_{1/2}\alpha$) of 0.38 h and an elimination half-life ($t_{1/2}\beta$) of 78.4 h (Table 1). The obtained $t_{1/2}\alpha$ is consistent to what was reported for paramagnetic quantum dot containing silica nanoparticles of similar size.[37] The long $t_{1/2}\beta$ indicates that not all the nanoparticles were cleared from the plasma within the 48 h sampling time. This is consistent with the measurements taken over the 8-week exposure time revealing appreciable levels of SiNPs in the plasma over the study period. These findings indicate that a portion of the dose remains in the plasma over an extended period of time, perhaps due to recirculation of SiNPs through enterohepatic circulation, or a delayed release of SiNPs from extrahepatic tissue back into the blood stream, resulting in a fraction of the dose having a long residence time.

The calculated mean pharmacokinetic parameters are presented in Table 1. Initial plasma concentration ($C_{initial}$) of ^{14}C-SiNPs was determined to be 154.0 μg/ml, and the mean plasma clearance rate (Cl) was calculated to be 18.2 ml/hr/kg. The apparent volume of distribution (V_d) was 2058.1 ml/kg. These values indicate a rapid and extensive distribution beyond the central compartment, which implies SiNPs must accumulate in organ tissues. Area under the curve (AUC) was calculated for intervals 0 to *t* and 0 to ∞ where *t* is the time of the last measurable concentration (48 h) and ∞ is infinity, using the linear trapezoidal method. The mean $AUC_{(0\text{-}t)}$ value was 445.5 μg-hr/ml, whereas the mean $AUC_{(0\text{-}\infty)}$ was 1099.4 μg-hr/ml. The greater than 2-fold increase in $AUC_{(0\text{-}\infty)}$ compared to $AUC_{(0\text{-}t)}$ is consistent with the long $t_{1/2}\beta$ indicating there was a significant level of nanoparticles remaining is the plasma beyond the 48 h sampling time. Applying a 2-compartment open model, the absorption rate of nanoparticles to the peripheral compartment from the central compartment (k_{12}) was 1.57 hr^{-1}. The k_{21} rate constant (transfer rate of nanoparticles from the peripheral compartment to the central compartment) was 0.11 hr^{-1}, and the elimination rate constant (k^{10}) was 0.14 hr^{-1}. The higher k_{12} compared to the k_{21} and k_{10} re-enforce the concept that the majority of the SiNP dose is rapidly eliminated from the plasma and distributed to tissues.

The sensitivity afforded by AMS allowed for the quantitative tissue distribution of SiNPs to be evaluated over an 8-week time course. Initial concentrations of SiNPs in tissue were assessed at time points of 0.25, 0.5, 1.0, 2.0, 8.0 and 24 hours after SiNP administration. Long-term distribution was determined at 1, 2, 7, 14, 28, 42 and 56 days post SiNP dosing. The results are reported as μg nanoparticles/gram of tissue in Table 2. For clarity, graphical representation of SiNP tissue concentration for liver, spleen, kidney, lung, and cervical lymph nodes, is depicted in Figure 2a and Figure 2b.

After IV administration, initial biodistribution of SiNPs was rapid and was confined primarily to tissues of the RES including the spleen, liver, kidney, lung, and cervical lymph nodes. There were also appreciable amounts detected in the bone marrow. The more peripheral tissue had much less accumulation of SiNPs. There was little or no distribution of SiNPs to the brain, muscle or adipose tissue. This is most likely due to the inability of the SiNPs to cross the blood brain barrier and the low blood perfusion rate in the striated muscle and adipose tissue, compared to the highly perfused organ tissues. Quantitative analysis revealed that the concentrations of SiNPS varied from tissue to tissue with the highest concentrations occurring in the spleen and liver, followed by lung and kidney. In all tissues examined, the Cmax concentration of SiNPs occurred within 2 h after dosing indicating a rapid distribution to the tissues. The spleen had the highest mean concentration of SiNPs at

298.6 μg/gm ± 43.4 at 2 hr post dose followed by the liver, kidney, and cervical lymph nodes at 228.2 μg/gm ± 7.46 and 56.91 μg/gm ± 13.6, and 33.9 μg/gm ± 9.11, respectively (Figure 2a). When adjusted to total tissue weight, at the Cmax, the liver contained the highest proportion of the dose at an average of 62% of the administered dose followed by the spleen, kidney and lung at 6.4%, 5.1%, and 1.5%, respectively. All other tissues contained less than 1% of the administered dose. These results are consistent with previous studies by Xie *et al.* who reported that both 20 nm and 80 nm SiNPs primarily accumulated in the spleen, liver, and lung, after a single IV dose of ^{125}I-SiNPs,[9] and Yu et al who showed a similar distribution profile from amine modified nonporous silica nanospheres. [24] Several other studies using qualitative techniques to detect SiNPs of various sizes and surface modifications confirm the results from this current study showing SiNPs accumulate primarily in the liver, spleen lung and bone marrow.[20–22, 37] In studies using immunohistochemical staining or confocal scanning laser microscopy, SiNPs ranging is size from 30–200 nm were located primarily in the macrophage of the liver, spleen and lung. [20, 37] In the lung, accumulation was also due to entrapment of the particles in the pulmonary vasculature.

Over the first 24 h after SiNP administration, the rate of change in SiNP concentration varied between tissues. In the liver, spleen, kidney, and lung, between 2–24 hr, the decrease in SiNP concentration ranged between 67–72%. In the cervical lymph nodes the concentration decreased by over 82% over the same time period. The bone marrow had the largest decrease in SiNP concentration of 87% from 0.25 h to 24 hr. The large decrease in the lymph tissue and bone marrow is consistent with the rapid elimination of the SiNPs from the plasma to the tissues. The concentrations of SiNPs within each tissue varied with time after administration. This could be attributed to the different capture rates of the various tissues and the level of circulating SiNPs in the blood and lymph.

Long-term biodistribution revealed that the overall trend was a gradual decline in SiNP levels in the tissues over time (Figure 2b). The data shows that, there was a significant amount of SiNPs remaining in the tissues 8 weeks after administration. In the kidney and lung, between 1 and 56 days after SiNP exposure, there was only a 20% decrease in SiNP concentration. In the liver and spleen there was a 72% and 57% decline in SiNP concentration, respectively, over the same time period (Table 2). The observed increase in SiNP tissue levels between 2 and 7 days was unexpected, but could be due to recirculation and redistribution of the SiNPs. The presence of SiNPS in the plasma and lymph tissue during this time reinforces this premise. Furthermore, in the lung, at 7 days post exposure the concentration of particles increased by 68% over the two-day concentration level and remained elevated through 14 days. In the spleen there was a similar increase between 14 and 28 days. The persistence of SiNPs in the tissues is most likely attributed to the uptake by macrophages residing within these tissues that are involved in the capture and metabolism of foreign particles and molecules.[9, 38] When nanoparticles are systemically administered, a variety of serum proteins can bind to their surface, which are recognized by the scavenger receptors on the macrophage cell surface and are removed from circulation.[39] Furthermore, the finding of SiNPs in the cervical lymph nodes and bone marrow, and their presence for up to 8 weeks suggest that there is the potential for an immune response from exposure to these SiNPs. In a similar study, Cho *et al.* showed that 50, 100 and 200 nm-sized SiNPs, when administered to mice IV, induced an inflammatory response in the liver and were retained in both the liver and spleen up to 4 weeks after dosing.[20] These current results together with previous studies demonstrate the importance of long term SiNP bioaccumulation and the potential effect it can have on tissue and cellular disposition. These factors need to be considered when assessing nanoparticles for biomedical and pharmaceutical applications. [40, 41]

Clearance of the SiNPs occurred through both the renal and biliary elimination routes (Figure 3). Of the total amount of SiNP excreted over the first 24 h of the study duration 69.4% was eliminated in the urine, whereas, 30.6% was found in the feces. In the urine the Cmax of 62.4 μg/ml occurred 2 hr post dose administration (Table 3). Clearance from the urine was rapid with a half-life ($T_{1/2}$) of 1.9 h and a clearance rate of 54.4 ml/hr/kg (Table 3). At 8 h only 12% of the Cmax concentration remained in the urine. Distribution to the feces was slower compared to the urine with the Cmax (22.1 μg/gm) occurring 8 h post dose administration. Elimination through the feces was also slower with a $T_{1/2}$ of 21 h and a clearance rate of 25.8 g/hr/kg. At 24 h post dose 49% of the Cmax concentration remained in the feces. These results indicate clearance through the urine is the primary route of elimination for the SiNPs. It is unlikely that elimination of SiNP via the urine is a result of glomerular filtration since the effective pore size of the glomerular wall is only 8 nm and the diameter of the SiNPs used in this study was 33 nm. It is most likely that the SiNPS were secreted into the urine by the mechanism of tubular secretion. The particles would have been secreted from the plasma directly through the epithelial cells lining the renal tubules into the tubular fluid. The endothelial cells contain fenestrations (pores) that are 70 to 90 nm in diameter, thus the 33 nm SiNPs could easily pass though the cells into the tubular fluid and be excreted.

Excretion by way of the fecal route goes through the liver and bile. It is well known that the liver has a high capacity to metabolize xenobiotics. The binding of proteins plays a key role in delivering xenobiotics from the plasma to the liver.[42] In addition the reticuloendothelial system can phagocytize particles then transport them to the liver, which can then be translocated to the bile and excreted in the feces. Chen *et al*. showed that when silica coated quantum dots had protein bound to their surface *in vivo*, or when they were aggregated to larger particles biliary excretion was favoured, and when the particles maintained their original nanosize without *in vivo* protein binding they were rapidly excreted via the kidney.[43] The finding from this current study, showing the presence of a significant amount of SiNPs in the feces is consistent with the particles having protein bound to them and/or being phagocytized into the liver. The aggregation of the particles could further lead to accumulation in the liver for which excretion would favor the biliary route.

In Conlcusion, this study was the first to use AMS to comprehensively quantify and track the biological fate of nanoparticles over an 8-week exposure period, and was the first to report both the PK and biodistribution of SiNPs *in vivo*. The *in vivo* biodistribution and PK parameters are important aspects for assessing the biosafety of nanomaterials. The biodistribution and PK profiles of nanomaterials are of essential significance for the investigation of tissue/organ toxicity, passive target capacities, and biomedical and pharmaceutical applications.[21] However, because of their small size it is very difficult to detect and track nanoparticles *in vivo*. Most studies that have investigated the *in vivo* biodistribution of SiNPs have been qualitative in nature.[20, 21, 23, 25] There are very few quantitative biodistribution studies and even fewer that assess the long-term kinetics of SiNPs *in vivo*.[9, 21] Results from this current study show that SiNPs were rapidly distributed to tissues of the RES and persisted in the tissue over the 8-week time course of the study. Excretion of SiNPs occurred by both the renal and biliary routes. The advantages of using AMS to determine the PK, biodistribution, and excretion characteristics on the SiNPs include the ability to determine long-term kinetics months after administration of SiNPs. Such a complete investigation would not be possible using other methods that lack the necessary sensitivity to detect compounds months after dosing. Detailed pharmacokinetic data require frequent sampling, which is also made possible with AMS detection, by virtue of the small sample sizes needed for analysis. Because of the high sensitivity and small sample size requirement, lower specific activity and less isotope were required for analysis which allowed for studies to be done at radiological doses that would not perturb the natural

physiological state of the organism. In addition, the use of AMS allows for future studies to be done at exposures that are environmentally or therapeutically relevant which makes it amenable to human tracer studies.

Acknowledgments

This work was performed under the auspices of the U.S. Department of Energy by, Lawrence Livermore National Laboratory at the Research Resource for Biomedical AMS under contract DE-AC52-07NA27344, and supported by grants from the National Institute of General Medical Sciences (8 P41 GM103483-14), and by Battelle Memorial Institute, CRADA No. PNNL/284.

References

1. Yang J, Lee J, Kang J, Lee K, Suh JS, Yoon HG, Huh YM, Haam S. Langmuir. 2008; 24(7):3417–21. [PubMed: 18324841]
2. Iezzi EB, Duchamp JC, Harich K, Glass TE, Lee HM, Olmstead MM, Balch AL, Dorn HC. J Am Chem Soc. 2002; 124(4):524–5. [PubMed: 11804475]
3. Zhao X, Hilliard LR, Mechery SJ, Wang Y, Bagwe RP, Jin S, Tan W. Proc Natl Acad Sci U S A. 2004; 101(42):15027–32. [PubMed: 15477593]
4. Hirsch LR, Stafford RJ, Bankson JA, Sershen SR, Rivera B, Price RE, Hazle JD, Halas NJ, West JL. Proc Natl Acad Sci U S A. 2003; 100(23):13549–54. [PubMed: 14597719]
5. Huo QS, Liu J, Wang LQ, Jiang YB, Lambert TN, Fang E. Journal of the American Chemical Society. 2006; 128:6447–6453. [PubMed: 16683810]
6. Roy I, Ohulchanskyy TY, Bharali DJ, Pudavar HE, Mistretta RA, Kaur N, Prasad PN. Proc Natl Acad Sci U S A. 2005; 102(2):279–84. [PubMed: 15630089]
7. Slowing, Trewyn BG, Lin VS. J Am Chem Soc. 2007; 129(28):8845–9. [PubMed: 17589996]
8. Lin W, Huang YW, Zhou XD, Ma Y. Toxicol Appl Pharmacol. 2006; 217(3):252–9. [PubMed: 17112558]
9. Xie G, Sun J, Zhong G, Shi L, Zhang D. Arch Toxicol. 2010; 84(3):183–90. [PubMed: 19936708]
10. Fischer HC, Chan WC. Curr Opin Biotechnol. 2007; 18(6):565–71. [PubMed: 18160274]
11. Colvin VL. Nat Biotechnol. 2003; 21(10):1166–70. [PubMed: 14520401]
12. Saffiotti U. Prog Clin Biol Res. 1992; 374:51–69. [PubMed: 1320275]
13. Merget R, Bauer T, Kupper HU, Philippou S, Bauer HD, Breitstadt R, Bruening T. Arch Toxicol. 2002; 75(11–12):625–34. [PubMed: 11876495]
14. Kirchner C, Liedl T, Kudera S, Pellegrino T, Munoz Javier A, Gaub HE, Stolzle S, Fertig N, Parak WJ. Nano Lett. 2005; 5(2):331–8. [PubMed: 15794621]
15. Choi HS, Liu W, Misra P, Tanaka E, Zimmer JP, Itty Ipe B, Bawendi MG, Frangioni JV. Nat Biotechnol. 2007; 25(10):1165–70. [PubMed: 17891134]
16. Kamps JA, Morselt HW, Swart PJ, Meijer DK, Scherphof GL. Proc Natl Acad Sci U S A. 1997; 94(21):11681–5. [PubMed: 9326670]
17. Krieger M, Herz J. Annu Rev Biochem. 1994; 63:601–37. [PubMed: 7979249]
18. Liu Z, Cai W, He L, Nakayama N, Chen K, Sun X, Chen X, Dai H. Nat Nanotechnol. 2007; 2(1): 47–52. [PubMed: 18654207]
19. Singh R, Pantarotto D, Lacerda L, Pastorin G, Klumpp C, Prato M, Bianco A, Kostarelos K. Proc Natl Acad Sci U S A. 2006; 103(9):3357–62. [PubMed: 16492781]
20. Cho M, Cho WS, Choi M, Kim SJ, Han BS, Kim SH, Kim HO, Sheen YY, Jeong J. Toxicol Lett. 2009; 189(3):177–83. [PubMed: 19397964]
21. He Q, Zhang Z, Gao F, Li Y, Shi J. Small. 2011; 7(2):271–80. [PubMed: 21213393]
22. Liu T, Li L, Teng X, Huang X, Liu H, Chen D, Ren J, He J, Tang F. Biomaterials. 2011; 32:1657–1668. [PubMed: 21093905]
23. He X, Nie H, Wang K, Tan W, Wu X, Zhang P. Anal Chem. 2008; 80(24):9597–603. [PubMed: 19007246]

24. Yu T, Hubbard D, Ray A, Ghandehari H. J Control Release. 2012; 163(1):46–54. [PubMed: 22684119]
25. Kumar R, Roy I, Ohulchanskky TY, Vathy LA, Bergey EJ, Sajjad M, Prasad PN. ACS Nano. 2010; 4(2):699–708. [PubMed: 20088598]
26. Vogel JS, Turteltaub KW, Finkel RC, Nelson DE. Anal Chem. 1995; 67:A353–A359.
27. Lappin G, Garner RC. Anal Bioanal Chem. 2004; 378(2):356–64. [PubMed: 14624324]
28. Turteltaub KW, Watkins BE, Vanderlaan M, Felton JS. Carcinogenesis. 1990; 11:43–49. [PubMed: 2403859]
29. Frantz CE, Bangerter C, Fultz E, Mayer KM, Vogel JS, Turteltaub KW. Carcinogenesis. 1995; 16:367–373. [PubMed: 7859370]
30. Dueker SR, Lin Y, Buchholz BA, Schneider PD, Lame MW, Segall HJ, Vogel JS, Clifford AJ. J Lipid Res. 2000; 41(11):1790–800. [PubMed: 11060348]
31. Wang W, Asher SA. J Am Chem Soc. 2001; 123(50):12528–35. [PubMed: 11741416]
32. Stöber W, Fink A, Bohn E. J Colloid Interface Sci. 1968; 26:62–69.
33. Creek MR, Mani C, Vogel JS, Turteltaub KW. Carcinogenesis. 1997; 18(12):2421–7. [PubMed: 9450490]
34. Ognibene TJ, Bench G, Vogel JS, Peaslee GF, Murov S. Anal Chem. 2003; 75(9):2192–6. [PubMed: 12720362]
35. Turteltaub KW, Felton JS, Gledhill BL, Vogel JS, Southon JR, Caffee MW, Finkel RC, Nelson DE, Proctor ID, Davis JC. Proc Natl Acad Sci USA. 1990; 87:5288–5292. [PubMed: 2371271]
36. Vogel JS. Radiocarbon. 1992; 34:333–350.
37. van Schooneveld MM, Vucic E, Koole R, Zhou Y, Stocks J, Cormode DP, Tang CY, Gordon RE, Nicolay K, Meijerink A, Fayad ZA, Mulder WJ. Nano Lett. 2008; 8(8):2517–25. [PubMed: 18624389]
38. Saba TM. Arch Intern Med. 1970; 126:1031–1052. [PubMed: 4921754]
39. Opanasopit P, Nishikawa M, Hashida M. Crit Rev Ther Drug Carrier Syst. 2002; 19(3):191–233. [PubMed: 12627613]
40. Li SD, Huang L. Mol Pharm. 2008; 5(4):496–504. [PubMed: 18611037]
41. Mamaeva V, Sahlgren C, Linden M. Adv Drug Deliv Rev. 2012
42. Levi AJ, Gatmaitan Z, Arias IM. J Clin Invest. 1969; 48(11):2156–67. [PubMed: 4980931]
43. Chen Z, Chen H, Meng H, Xing G, Gao X, Sun B, Shi X, Yuan H, Zhang C, Liu R, Zhao F, Zhao Y, Fang X. Toxicol Appl Pharmacol. 2008; 230(3):364–71. [PubMed: 18495192]

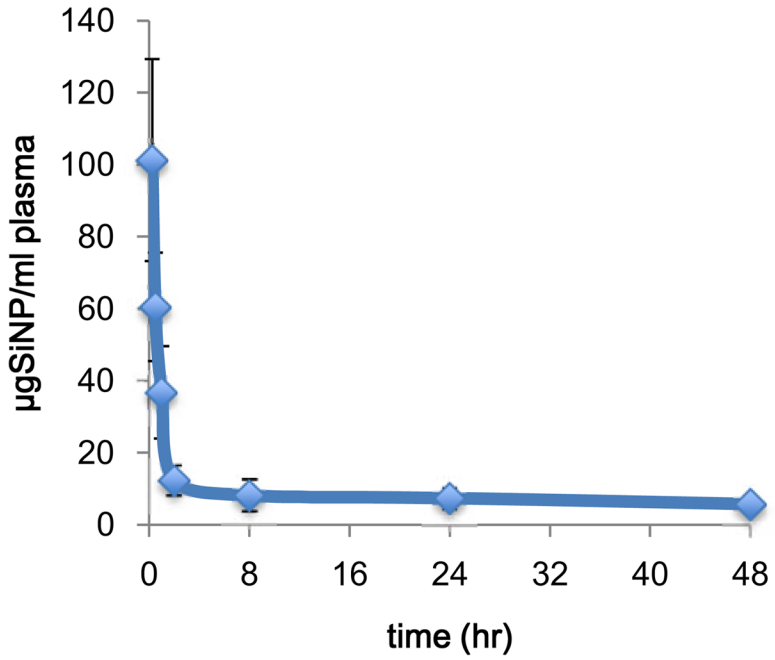

Figure 1.

Mean plasma concentration versus time curve of ^{14}C-SiNP (33 nm), following single 0.5 mg intravenous administration to BALB/c male mice. Results are the mean of 5 animals ± the standard error of the mean.

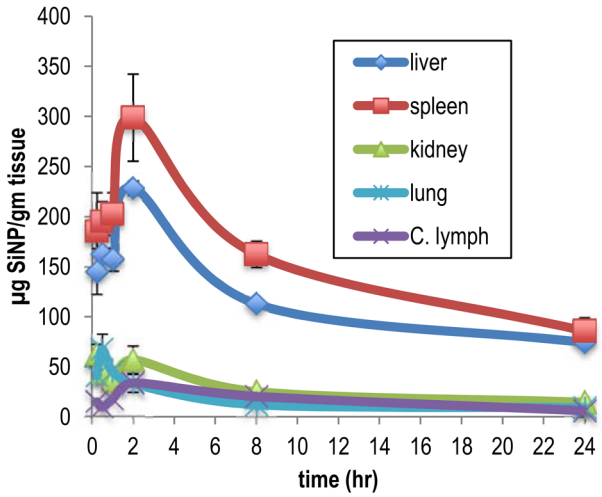

Figure 2a.

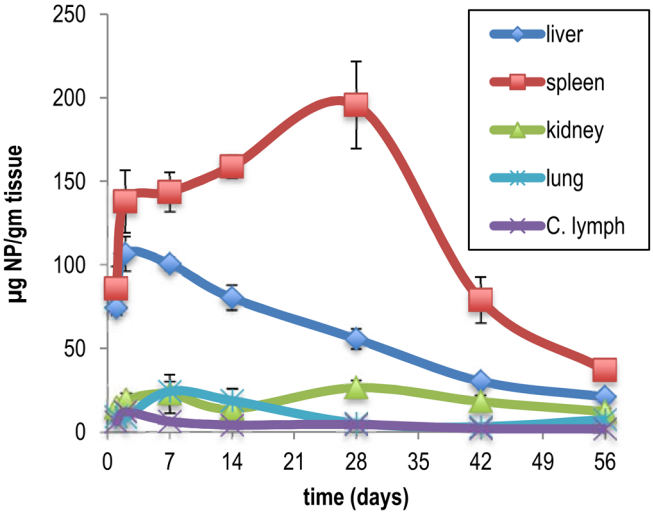

Figure 2b.

Figure 2.

Figure 2a. Mean tissue concentration of ^{14}C-SiNP (33 nm), over a 24 h sampling time, following single 0.5 mg intravenous administration to BALB/c male mice. Data are expressed as the mean of 5 animals ± the standard error of the mean.

Figure 2b. Mean tissue concentration of ^{14}C-SiNP (33 nm), over a 56 day sampling time, following single 0.5 mg intravenous administration to BALB/c male mice. Data are expressed as the mean of 5 animals ± the standard error of the mean.

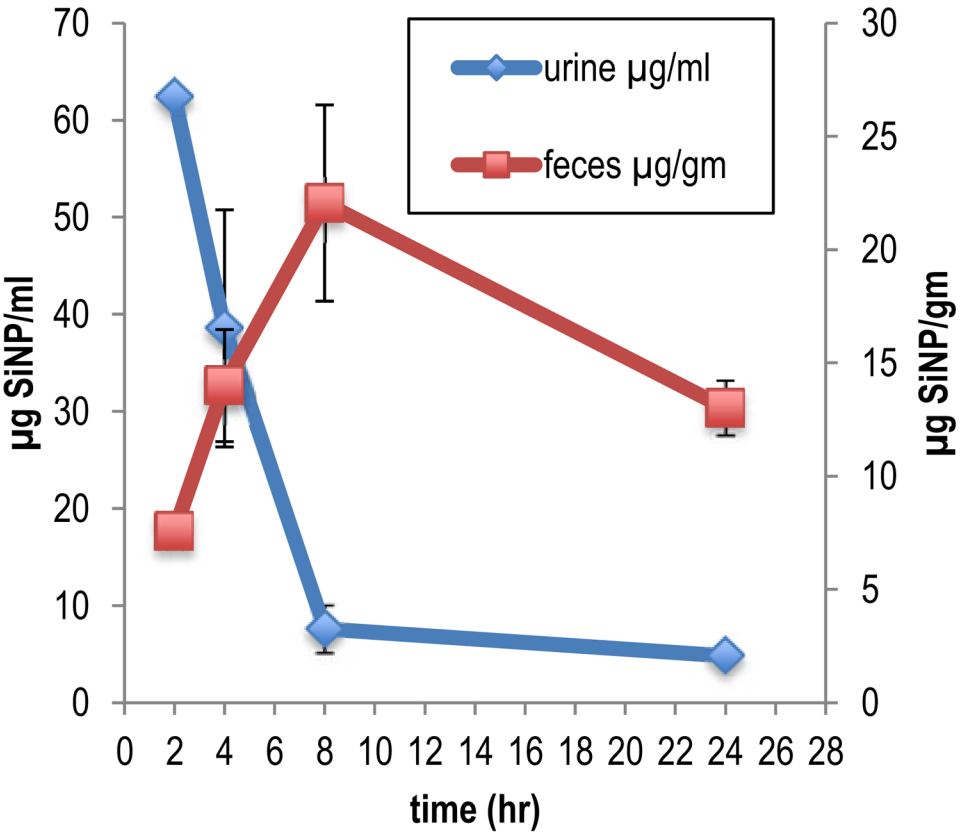

Figure 3.
Mean concentration of ^{14}C-SiNP (33 nm) in urine and feces, over a 24 h sampling time, following single 0.5 mg intravenous administration to BALB/c male mice. Data are expressed as µg of ^{14}C-SiNP/ml of urine and µg of ^{14}C-SiNP/gm of feces. Results are the mean of 5 animals ± the standard error of the mean.

Table 1

Mean plasma pharmacokinetic parametersof SiO_2 nanoparticles following a single intravenous administration of 0.5 mg ^{14}C-SiO_2 nanoparticles to male BALB/c mice

Dose	**Mg**	**0.5**
$C_{(initial)}$	μg/mL	154.0
$t_{1/2}$ a	hr	0.38
$t_{1/2}$ b	hr	78.4
$AUC_{0\text{-}t}$	μg-hr/mL	445.5
$AUC_{0\text{-}\infty}$	μg-hr/mL	1099.4
CL	mL/hr/kg	18.2
V_d	mL/kg	2058.1
V_{ss}	ml	46.8
k_{12}	hr^{-1}	1.58
k_{21}	hr^{-1}	0.11
k_{10}	hr^{-1}	0.14

Table 2

Mean tissue concentration of ^{14}C-SiNP (33 nm), over time (0–24 h), following a single 0.5 mg intravenous administration to male BALB/c mice

	μg SiO_2 nanoparticles/gm tissue ± SEM					
	0.25 hr	**0.5 hr**	**1.0 hr**	**2.0 hr**	**8 hr**	**24 hr**
Liver	145.24 ± 22.96	162.43 ± 2.61	157.52 ± 1.41	228.20 ± 7.46	112.81 ± 4.41	74.21 ± 4.58
Spleen	185.14 ± 38.46	195.07 ± 20.1	202.29 ± 21.3	298.65± 43.4	162.15 ± 13.4	85.64 ± 13.33
Kidney	63.07 ± 9.09	45.10 ± 2.56	35.91 ± 8.8	56.91 ± 13.6	25.11 ± 2.39	14.66 ± 1.16
Lung	41.12 ± 4.05	67.22 ± 15.20	45.05 ± 4.43	33.11 ± 9.11	12.12 ± 2.22	9.02 ± 2.59
Heart	17.47 ± 2.6	12.35 ± 1.1	6.43 ± 1.41	13.26 ± 4.46	6.05 ± 0.11	5.31 ± 0.57
Colon	3.43 ± 0.43	2.65 ± 0.89	2.14 ± 0.65	5.44 ± 2.66	1.80 ± 0.25	0.88 ± 0.16
Upper gi	6.04 ± 1.65	5.76 ± 2.42	2.66 ± 0.38	6.56 ± 1.21	5.20 ± 1.89	3.96 ± 3.67
Muscle	1.57 ± 0.34	0.95 ± 0.10	0.53 ± 0.06	1.18 ± 0.51	0.50 ± 0.07	0.47 ± 0.14
Adipose	8.37 ± 1.22	4.64 ± 0.66	3.13 ± 1.02	3.59 ± 0.93	1.22 ± 0.2	0.70 ± 0.34
Brain	1.45 ± 0.39	0.94 ± 0.39	0.53 ± 0.14	0.72 ± 0.37	0.08 ± 0.01	0.03 ± 0.01
Bone marrow	43.99 ± 10.4	6.56 ± 2.24	10.20 ± 5.14	9.38 ± 3.46	4.79 ± 1.25	5.54 ± 2.25
Cervical lymph	14.94 ± 5.62	9.64 ± 1.19	17.43 ± 9.15	33.92 ± 6.62	20.47 ± 10.02	6.08 ± 0.59

Mean tissue concentration of ^{14}C-SiNP (33 nm), over time (1–56 days), following a single 0.5 mg intravenous administration to male BALB/c mice

	μg SiO_2 nanoparticles/gm tissue ± SEM						
	1 day	**2 day**	**7 days**	**14 days**	**28 days**	**42 days**	**56 days**
Liver	74.21 ± 4.58	106.7 ± 10.3	100.5 ± 4.09	80.23 ± 7.59	55.57 ± 6.26	30.23 ± 3.25	20.99 ± 1.69
Spleen	85.64 ± 13.3	137.9 ± 18.7	143.5 ± 11.7	158.75 ± 6.7	195.6 ± 26.1	78.96 ± 13.6	36.93 ± 2.71
Kidney	14.66 ± 1.16	19.40 ± 3.78	22.7 ± 11.48	13.67 ± 1.57	26.38 ± 4.51	18.1 ± 3.84	12.11 ± 1.81
Lung	9.02 ± 2.59	8.68 ± 0.57	24.33 ± 5.67	18.78 ± 6.95	5.14 ± 1.84	3.09 ± 0.44	7.40 ± 1.48
Heart	5.31 ± 0.57	5.78 ± 0.31	1.27 ± 0.16	0.86 ± 0.11	1.27 ± 0.37	0.68 ± 0.05	0.43 ± 0.03
Colon	0.88 ± 0.16	1.34 ± 0.15	1.01 ± 0.36	0.39 ± 0.11	2.75 ± 1.99	0.94 ± 0.091	0.68 ± 0.12
Upper gi	3.96 ± 3.67	3.43 ± 1.45	1.20 ± 0.15	0.90 ± 0.14	16.27 ± 7.54	6.29 ± 2.04	4.65 ± 1.16
Muscle	0.47 ± 0.14	0.30 ± 0.06	0.38 ± 0.14	0.23 ± 0.05	0.23 ± 0.06	0.16 ± 0.02	0.14 ± 0.01
Adipose	0.70 ± 0.34	1.05 ± 0.33	1.09 ± 0.76	0.22 ± 0.10	1.32 ± 0.18	3.48 ± 0.28	2.93 ± 0.31
Brain	0.03 ± 0.009	0.06 ± 0.003	0.32 ± 0.15	0.07 ± 0.02	0.06 ± 0.01	0.32 ± 0.04	0.29 ± 0.01
Bone marrow	5.54 ± 2.25	11.55 ± 6.31	12.45 ± 2.31	4.41 ± 0.86	0.85 ± 0.14	1.51 ± 0.48	2.17 ± 1.4
Cervical lymph	6.08 ± 0.59	12.05 ± 6.61	6.35 ± 4.15	4.14 ± 1.38	4.42 ± 1.47	1.97 ± 0.54	1.82 ± 0.66

Table 3

Mean (n=5) excretion kinetics of SiO_2 nanoparticles following a single intravenous administration of 0.5 mg ^{14}C-SiO_2 nanoparticles to male BALB/c mice

Elimination route	$C_{(max)}$	$T_{(max)}$ (h)	$t_{1/2}$ (h)	CL (mL/h/kg)
urine	62.4 μg/ml	2.0	1.9	54.4
feces	22.0 μg/gm	8.0	22.1	25.8